Transnational University Limburg is a unique collaboration of two universities in two countries: the University of Hasselt and Maastricht University.

UHASSELT
KNOWLEDGE IN ACTION

www.uhasselt.be
Universiteit Hasselt
Campus Hasselt:
Martelarenlaan 42 | 3500 Hasselt
Campus Diepenbeek:
Agoralaan Gebouw D | 3590 Diepenbeek

UHASSELT
KNOWLEDGE IN ACTION

Maastricht University

Faculty of Medicine and Life Sciences
School for Life Sciences
Master of Biomedical Sciences

Master's thesis

A mechanistic link between diabetes and cardiovascular risk: the impact of methylglyoxal-driven neutrophil activation

Marie-Lore Vrancken

Thesis presented in fulfillment of the requirements for the degree of Master of Biomedical Sciences, specialization Molecular Mechanisms in Health and Disease

SUPERVISOR :

Prof. dr. Kristiaan WOUTERS

2025
2026

Maastricht University

Faculty of Medicine and Life Sciences
School for Life Sciences
Master of Biomedical Sciences

Master's thesis

A mechanistic link between diabetes and cardiovascular risk: the impact of methylglyoxal-driven neutrophil activation

Marie-Lore Vrancken

Thesis presented in fulfillment of the requirements for the degree of Master of Biomedical Sciences, specialization Molecular Mechanisms in Health and Disease

SUPERVISOR :

Prof. dr. Kristiaan WOUTERS

A mechanistic link between diabetes and cardiovascular risk: the impact of methylglyoxal-driven neutrophil activation. *

Marie-Lore Vrancken[1], Yu Oshima[2], Jean Scheijen[2], Rory Koenen[3], Casper Schalkwijk[2], and Kristiaan Wouters[2]

[1]Biomedical Sciences, Faculty of Medicine and Life Sciences, Hasselt University, Campus Diepenbeek,
Agoralaan Building D – 3590 Diepenbeek, Belgium
[2]Internal Medicine, Cardiovascular Research Institute Maastricht, Universiteit Maastricht,
Universiteitssingel 40 – 6200 Maastricht, The Netherlands
[3]Biochemistry, Cardiovascular Research Institute Maastricht, Universiteit Maastricht,
Universiteitssingel 40 – 6200 Maastricht, The Netherlands

**The effect of MGO on neutrophil activation.*

To whom correspondence should be addressed: Kristiaan Wouters, Tel: 043 38 84233; Email: kristiaan.wouters@maastrichtuniversity.nl

Keywords: methylglyoxal, diabetes, cardiovascular risk, neutrophils, inflammation, atherosclerosis

ABSTRACT

Diabetes mellitus is a chronic metabolic disorder characterized by hyperglycemia, which damages vasculature and increases the risk of cardiovascular disease (CVD). While vascular inflammation is a hallmark of CVD, the mechanisms linking hyperglycemia to this response remain partly understood. Methylglyoxal (MGO), a highly reactive glycolytic byproduct, is a potential mediator due to its ability to stimulate inflammation by inducing oxidative stress and promoting advanced glycation end product formation. Neutrophils are among the first immune cells recruited to sites of vascular injury and play a key role in inflammation. However, excessive activation can cause tissue damage through NETosis, a process in which neutrophil extracellular traps (NETs) are released. This study investigated whether MGO drives neutrophil activation, and if pharmacological intervention can attenuate MGO levels. Human neutrophils were isolated and stimulated with phorbol 12-myristate 13-acetate (PMA). Intracellular MGO levels were quantified by flow cytometry and confirmed by mass spectrometry. NETosis and MGO localization were assessed using microscopy. PMA stimulation induced a time-dependent accumulation of MGO, reaching peak levels after 4 hours and coinciding with increased NETosis. Although aminoguanidine reduced MGO levels, it failed to suppress NET formation. In contrast, resveratrol and hesperetin, particularly in combination with pyridoxamine, significantly reduced both MGO levels and NETosis. Furthermore, MGO spatially redistributed during NETosis and did not colocalize with MPO. These findings identify MGO accumulation as a contributor to neutrophil activation, while additional pathways, including oxidative stress, are likely involved. A synergistic MGO-scavenging strategy may represent a promising therapeutic approach for reducing cardiovascular risk in diabetes.

INTRODUCTION

Diabetes mellitus is a chronic metabolic disorder with a rapidly increasing global prevalence and represents a major cause of morbidity and mortality worldwide. Currently, approximately one in nine adults is affected, and this number is expected to rise further in the coming decades (1-3). The rising prevalence of diabetes is driven by multiple factors, including population aging, socioeconomic and lifestyle changes associated with economic development, and improved medical management that increases survival and prolongs the disease duration (4). Diabetes is characterized by persistently elevated blood glucose levels (hyperglycemia) due to impaired insulin production, insulin resistance, or a combination of both (2). The most common forms are type 1 diabetes and type 2 diabetes. Type 1 diabetes is an autoimmune disease in

which pancreatic β-cells are destroyed, leading to insulin deficiency. Type 2 diabetes, conversely, is primarily caused by insulin resistance, often accompanied by inadequate insulin secretion (2). Other forms include gestational diabetes, prediabetes, and secondary diabetes, which result from other medical conditions or medications, such as type 3c diabetes, which develops due to pancreatic damage (2). Chronic hyperglycemia in diabetes is associated with both acute complications and progressive damage to various organ systems. The most significant consequences include microvascular and macrovascular complications, which contribute to reduced quality of life and premature mortality. Microvascular dysfunction affects small vessels in the retina, kidneys, and peripheral nerves, leading to diabetic retinopathy, nephropathy, and neuropathy, respectively. In parallel, diabetes accelerates macrovascular disease, primarily through an enhanced progression of atherosclerosis. This process involves the coronary, carotid, and peripheral arteries. Among these complications, atherosclerotic cardiovascular disease (CVD) represents one of the most significant macrovascular complications in diabetes (5).

CVD encompasses all disorders affecting the heart or the blood vessels (6). Atherosclerotic CVD, a major subset, is characterized by the accumulation of lipid-rich plaques within the arterial wall, leading to progressive narrowing, vascular stiffening, impaired blood flow, and plaque rupture (7, 8). Damage to the vasculature can cause organ dysfunction in the brain, heart, kidneys, and eyes due to reduced delivery of oxygenated blood. These events can result in acute events such as myocardial infarction, ischemic stroke, transient ischemic attacks, peripheral arterial disease, and aortic disease (7, 8). Diabetes and hyperglycemia substantially increase the risk of CVD by damaging the vascular endothelium, promoting inflammation, and accelerating plaque formation (7-10). Current therapeutic strategies for diabetes focus on lifestyle modifications and medications, primarily consisting of statins for lipid management. These approaches reduce the risk of developing macrovascular diabetes complications. However, they do not fully prevent CVD, and a substantial residual risk of approximately 30% remains (11). Given that atherosclerosis is inherently an inflammatory process, targeting inflammation has emerged as a potential strategy. However, the clinical application of broad anti-inflammatory agents has proven to be complex. Large-scale clinical trials have demonstrated that systemic immune suppression can be inconsistent in its efficacy and is often associated with significant side effects, most notably an increased risk of serious infections (12, 13). This highlights the need for more selective therapies. Rather than suppressing the entire immune response, a more effective approach may lie in targeting the specific upstream metabolic drivers that trigger inflammation. **However, the mechanistic link between hyperglycemia and vascular inflammation is not yet fully understood.**

One potential mediator of this link involves **methylglyoxal (MGO)**, a highly reactive dicarbonyl metabolite (14, 15). MGO is associated not only with hyperglycemia, but also with other cardiometabolic risk factors such as hypertension, dyslipidemia, incident CVD, and obesity (15). It is primarily generated as a byproduct of glycolysis through the spontaneous decomposition of the triose phosphates dihydroxyacetone phosphate (DHAP) and glyceraldehyde-3-phosphate (G3P) (Fig. 1). Under physiological conditions, the chemical instability of DHAP and G3P can lead to non-enzymatic release of the phosphate group, yielding MGO. MGO is found in higher intracellular concentrations compared to extracellular levels, possibly due to higher levels of unstable reversibly bound MGO to cellular proteins (16). In normal conditions, MGO is detoxified to D-lactate through the glyoxalase system, including glyoxalase 1 (GLO1) and glyoxalase 2 (GLO2). However, under hyperglycemic conditions, excessive glucose metabolism increases MGO formation beyond the cell's detoxification capacity or decreases the functioning of the glyoxalase system, leading to MGO accumulation (17, 18). This contributes to vascular pathology both directly and indirectly. Directly, MGO enhances oxidative stress and activates pro-inflammatory signaling cascades such as nuclear factor-kB (NF-kB) (14, 19, 20). Indirectly, MGO promotes the formation of advanced glycation end products (AGEs) that bind to their receptor, RAGE, leading to irreversible glycation of mitochondrial proteins, lipids, and nucleic acids (14, 19, 20). This

signaling cascade impairs cellular function by inhibiting DNA synthesis and altering mitochondrial integrity. It also increases vascular permeability, and it promotes pathological angiogenesis and pro-thrombotic responses (14, 19, 20). MGO-derived AGEs accumulate in atherosclerotic plaques, stimulating plaque inflammation, necrotic core formation, and plaque instability, events that contribute to cardiovascular complications in diabetes (15, 21). Despite these findings, **the precise molecular pathways that link MGO accumulation to vascular inflammation and cardiovascular risk are poorly defined**.

In addition, in the vascular complications of diabetes, immune dysregulation plays a central role, with **neutrophils** emerging as key mediators (22). Tissue injury, including cardiac injury and atherosclerosis, rapidly triggers the recruitment of innate immune cells to sites of damage to clear debris and dead cells. This process is initiated through pattern recognition receptors (PRR), like toll-like receptors, that detect damage-associated molecular patterns or pathogen-associated molecular patterns (23). PRR engagement activates neutrophils and induces downstream signaling cascades, including transcriptional activation of NF-kB. This leads to increased inflammatory gene transcription and cytokine production (24). Hyperglycemia promotes neutrophil expansion and proliferation, thereby amplifying inflammatory responses (25). Neutrophils exhibit a distinct metabolic profile characterized by a strong dependence on glycolysis for energy production. In addition, the pentose phosphate pathway, which uses intermediates of the glycolysis to produce nicotinamide adenine dinucleotide phosphate (NADPH) for reactive oxygen species (ROS) production, also facilitates neutrophil function (9, 26, 27). In contrast, mitochondrial oxidative phosphorylation and fatty acid oxidation play a limited role in ATP generation in neutrophils (26, 27). Hyperglycemia markedly alters this metabolic balance by increasing glycolytic flux to meet elevated energy demands. Furthermore, it also primes neutrophils toward a pro-inflammatory phenotype characterized by increased ROS production, enhanced degranulation, phagocytosis, and elevated neutrophil extracellular trap (NET) formation through a process known as NETosis (28-30). Based on these metabolic and functional features, we hypothesize that MGO production may contribute to neutrophil function under hyperglycemic conditions. While neutrophils are known targets of hyperglycemia-induced oxidative stress, **their potential contribution to MGO accumulation remains largely unexplored**. Given their high glycolytic activity and short lifespan, neutrophils may represent an underappreciated cellular source of MGO under hyperglycemic conditions (31).

One of the characterizations of neutrophil activation is **NETosis**. This is an antimicrobial defense mechanism in which neutrophils expel intracellular material into the extracellular space as NETs. This process involves disassembly of the nuclear envelope, citrullination of histones, and chromatin decondensation, followed by permeabilization of the plasma membrane and expulsion of chromatin decorated with granular proteases into the extracellular space (32-34). Under physiological conditions, NET formation is tightly regulated, however, it becomes exaggerated in diabetes due to increased ROS levels, carbonyl stress, and mitochondrial dysfunction (28, 29, 35). Dysregulated NET formation results in the release of cytotoxic and pro-inflammatory components, including histones, myeloperoxidase (MPO), neutrophil elastase (NE), and extracellular DNA, which directly damage endothelial and vascular smooth muscle cells (34). In addition, these components also act as scaffolds for platelet adhesion and fibrin deposition, thereby promoting thrombosis and accelerating atherosclerotic lesion development (28, 29). At the tissue level, NETs and neutrophil-derived proteases degrade extracellular matrix proteins, disrupt endothelial junctions, and enhance permeability. Concurrent activation of endothelial and platelet coagulation pathways, together with macrophage inflammasome activation, leads to cytokine release (29, 35). These combined events drive plaque inflammation, expansion of the necrotic core, and destabilization of atherosclerotic lesions, ultimately leading to plaque rupture (29). Notably, experimental inhibition of NET formation or acceleration of NET clearance reduces atherosclerotic inflammation in preclinical diabetic models, supporting a causal role for neutrophil overactivation in atherothrombosis (29).

Despite growing evidence, there remain significant knowledge gaps regarding the connection between hyperglycemia, MGO metabolism, and neutrophil activation. This represents a crucial missing link between diabetes and cardiovascular risk.

In order to investigate the impact of MGO on neutrophil function, we used several MGO inhibition strategies. In recent years, reactive carbonyls have emerged as important mediators of diabetic complications and have gained increasing attention as potential therapeutic targets (27). As a result, several compounds capable of quenching MGO have been identified and evaluated. In this study, aminoguanidine (AG) was selected as a pharmacological tool to modulate MGO-related pathways. Later, we also investigated a cocktail of pyridoxamine (Pyr), resveratrol (Res), and hesperitin (Hes) to reduce MGO levels. In parallel, phorbol 12-myristate 13-acetate (PMA) was used to induce controlled neutrophil activation.

Phorbol 12-myristate 13-acetate (PMA) is a widely used experimental stimulus for inducing neutrophil activation and NET formation. This phorbol ester acts as a diacylglycerol analog and directly activates protein kinase C, thereby triggering downstream signaling pathways involved in neutrophil degranulation, metabolic reprogramming, ROS production, and NETosis. These processes involve key effector molecules such as MPO and NE. Although PMA represents an artificial stimulus that does not fully recapitulate physiological neutrophil activation, it provides a robust and reproducible tool to interrogate intracellular signaling mechanisms underlying neutrophil activation (36). In this context, PMA-induced neutrophil activation enables controlled investigation of how metabolic stressors, such as MGO, influence neutrophil inflammatory responses relevant to diabetic vascular disease.

Aminoguanidine (AG) is a nucleophilic hydrazine compound with multiple biological actions relevant to diabetes and its vascular complications. It is primarily known for its antiglycation activity, acting as an inhibitor of AGE formation by reacting with early glycosylation products. Through this mechanism, AG will prevent their conversion into stable, cross-linked AGEs on proteins and extracellular matrix components. AG markedly inhibits AGE formation on model proteins such as collagen and albumin, and is widely used as a reference antiglycation agent in experimental systems (37, 38). Beyond its antiglycation effects, AG also exhibits antioxidant and immunomodulatory properties. It has been shown to attenuate oxidative stress and modulate inflammatory responses in various experimental systems, partly through inhibition of ROS generation. In addition, AG has been reported to increase neutrophil NADPH oxidase (NOX2) activity, through activation of PKC, and microbicidal function, suggesting that it may directly influence innate immune cell function (37, 39, 40). In preclinical models of diabetic complications, AG attenuates AGE accumulation, reduces vascular permeability, and limits fibrotic tissue remodeling in organs such as the kidney and the heart (41, 42). However, its clinical translation has been limited because of safety concerns and apparent lack of efficacy (37, 38). Despite these well-characterized actions**, the direct effect of AG on MGO levels and MGO-mediated processes**, particularly within immune cells such as neutrophils, **remains unclear**.

In addition to AG, several other compounds with carbonyl-scavenging and antiglycation properties have been identified, including **Pyr, Res, and Hes** (43-46). Pyr, a vitamin B6 derivative, inhibits AGE formation by trapping reactive carbonyl intermediates generated during carbohydrate and lipid degradation and by inhibiting oxidative steps in carbonyl-mediated protein modification (43, 44). However, prior studies within our research department did not demonstrate significant effects when Pyr was used as a single agent (data not provided). In contrast, a marked reduction in MGO and AGE levels was observed when Pyr was combined with resveratrol and hesperitin, suggesting additive or synergistic carbonyl-quenching effects (data not provided). Res is a polyphenolic flavonoid with well-documented antioxidant, anti-inflammatory, and cardioprotective properties, mediated through modulation of redox signaling and inflammatory pathways (45). Hes, another bioactive flavonoid, also exhibits anti-oxidative and anti-inflammatory activity and has been shown to inhibit AGE formation through both radical scavenging and carbonyl-

trapping mechanisms (46). However, despite these well-characterized individual mechanisms of action, the **combined effects of this multi-compound cocktail on MGO metabolism and immune cell function remain insufficiently defined**.

In **summary**, chronic hyperglycemia induces significant metabolic and inflammatory alterations that lead to MGO accumulation, immune cell dysfunction, and vascular injury. Despite increasing evidence for the involvement of MGO and neutrophils in diabetic cardiovascular complications, its downstream effects within neutrophils remain poorly understood. Addressing these knowledge gaps is essential to better understand the persistent cardiovascular risk in diabetes. Therefore, this thesis aims to investigate whether MGO production in neutrophils modulates neutrophil inflammatory responses relevant to atherosclerotic cardiovascular disease. Furthermore, we evaluated the efficacy of pharmacological interventions, specifically AG, a multi-compound cocktail including Res, Hes, and Pyr, and its separate components, in attenuating MGO levels. To achieve this, neutrophils were isolated from human blood, stimulated using PMA, and treated. We hypothesize that 1) human neutrophils produce MGO after activation and thereby promote pro-inflammatory activity by inducing NETosis, and 2) that pharmacological intervention can effectively reduce intracellular MGO levels, thereby mitigating neutrophil-driven inflammatory signaling.

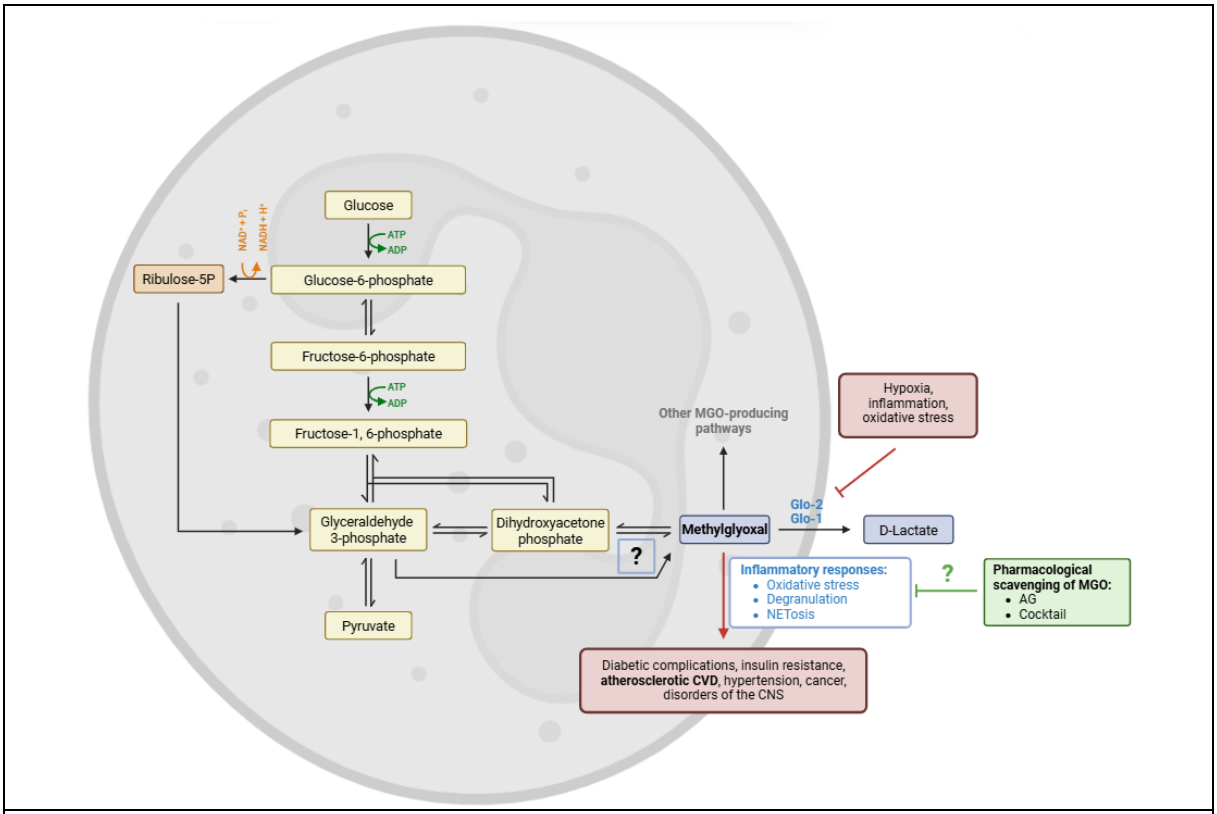

Fig. 1 – Metabolic pathways of methylglyoxal (MGO) formation and its pathological outcomes in neutrophils. Illustration of metabolic origin and downstream inflammatory effects of MGO within a human neutrophil under hyperglycemic stress. Methylglyoxal is primarily derived from the spontaneous degradation of triose phosphate intermediates. While the glyoxalase enzymes (Glo-1, Glo-2) convert MGO to D-lactate, inhibitory factors can lead to MGO accumulation. Elevated MGO levels in neutrophils trigger inflammatory responses, contributing to chronic conditions such as diabetic complications and atherosclerotic CVD. This thesis aims to determine how MGO accumulation modulates neutrophil-specific pro-inflammatory responses (?), and evaluate the efficacy of pharmacological scavengers in attenuating MGO-driven vascular inflammation (?). *MGO, methylglyoxal; ATP, adenosine triphosphate; ADP, adenosine diphosphate; Glo, glyoxalase; NETosis, neutrophil extracellular trap formation; CVD, cardiovascular disease; CNS, central nervous system; AG, aminoguanidine.*

EXPERIMENTAL PROCEDURES

Neutrophil isolation – Human neutrophils were isolated from peripheral blood obtained from healthy volunteers by density-gradient centrifugation. Venous blood was collected by venipuncture into 10 ml EDTA-coated tubes (BD life sciences) under sterile conditions. All subsequent steps were also performed using sterile techniques. To sediment erythrocytes, whole blood was mixed 1:1 (v/v) with a 3% (w/v) Dextran-500 solution (Carl Roth GmbH + Co KG.) prepared in 0.9% NaCl (Merck) and allowed to stand at room temperature for 30 minutes. Following sedimentation, the leukocyte-rich supernatant was carefully collected, washed with phosphate-buffered saline (PBS; Gibco, Thermo Fisher Scientific), and resuspended in PBS. The cell suspension was subsequently layered onto a discontinuous Percoll density gradient consisting of 85%, 80%, 75%, 70%, and 65% (v/v) Percoll (Sigma-Aldrich) solutions, with the highest density layer at the bottom. Gradient centrifugation was performed for 20 minutes at 800 x g at room temperature without brake. After centrifugation, the neutrophil-enriched fraction was collected, washed with PBS, and resuspended in culture medium consisting of RPMI 1640 GlutaMAX™ (Gibco), supplemented with 25 mM HEPES (Sigma-Aldrich) and 1% heat-inactivated fetal calf serum (iFCS) (TICO Europe). Isolated neutrophils were counted using Trypan blue and a Bürker-Türk counting chamber.

Neutrophil treatment and stimulation – For the measurement of intracellular MGO formation by flow cytometry or mass spectrometry and the assessment of NETosis, freshly isolated neutrophils were cultured in culture medium (RPMI 1640 GlutaMAX™ medium, 25 mM HEPES, 1% iFCS). Cells were seeded at a density of 3 x 10^5 cells per well in either 96-well plates (flow cytometry, mass spectrometry) or 24-well plates (NETosis assay). To detect intracellular MGO with flow cytometry, neutrophils were incubated with the methyl diaminobenzene-BODIPY (MBo) probe (47) at final concentrations of 0.5, 1, 2.5, 5, or 10 µM. All cells were pre-incubated, with or without the probe, for 1 hour in the dark. Subsequently, cells were washed twice with PBS and resuspended in fresh culture media before further treatment. To investigate MGO scavenging, 5 mM aminoguanidine (AG; Sigma-Aldrich), 100 µM resveratrol (Res), 50 µM hesperetin (Hes), or 500 µM pyridoxamine (Pyr) was added 30 minutes prior to stimulation. For short-term stimulation, neutrophils were treated with 50 nM phorbol 12-myristate 13-acetate (PMA; Merck) dissolved in Dimethyl Sulfoxide (DMSO). PMA stimulation was performed for 20 minutes to 5 hours for flow cytometric analyses, mass spectrometry, and NETosis assays.

Flow cytometry – Flow cytometric analysis using the Aurora flow cytometer (Cytek Biosciences) was performed to quantify intracellular MBo fluorescence as a measure of MGO formation. Following treatment and stimulation, neutrophils were incubated with Zombie NIR™ viability dye for 15 minutes at room temperature in the dark. Cells were then washed with PBS, resuspended in a fluorescence-activated cell sorting (FACS) buffer, and analyzed using an Aurora spectral flow cytometer using the FITC, Zombie NIR, and zombie UV channels. Neutrophils were identified based on side scatter (SSC) and forward scatter (FSC) characteristics. Cell viability was determined using the Zombie NIR signal and FSC/SSC gating (Fig. S1) and expressed as the percentage of viable cells relative to the parent population. MBo-positive cells were identified based on MBo intensity and quantified as the median FITC-A intensity within the singlet cell gate. The data was analyzed using the SpectroFlo software (Cytek Biosciences)

NETosis assay – NET formation was assessed by immunofluorescence or confocal microscopy. Following treatment and stimulation, neutrophils were fixed with 2% formaldehyde (Sigma-Aldrich). Cells were then washed three times with PBS or demineralized water and permeabilized using 0.5% Triton X-100 (Sigma-Aldrich). After an additional three washing steps, nonspecific binding was blocked by incubation with Roti-ImmunoBlock 1x (Carl Roth) for 30 minutes at 37°C in a humid chamber. Cells were subsequently incubated with primary antibody anti-myeloperoxidase (Sigma-Aldrich), followed by a washing step and incubation with an appropriate secondary antibody, donkey anti-rabbit-Alexa Fluor 647 (Sigma-Aldrich). NETs were visualized by nuclear staining with 10 µg/ml DAPI (Carl Roth) in mounting medium (Carl Roth). Images

of NETosis were acquired using an EVOS M5000 fluorescence microscope (Thermo Fisher Scientific; 20x magnification). NETosis was quantified by manual counting and expressed as the percentage of NETosis-positive cells relative to the total number of visible neutrophils per field. The localization of MGO in neutrophils was determined using a LEICA TCS SP8 STED confocal microscope (Leica Microsystems; 25x and 85x magnification).

Mass Spectrometry – Ultraperformance liquid chromatography tandem mass spectrometry (UPLC-MS/MS) was performed to analyze the intracellular MGO levels. Following neutrophil treatment and stimulation, approximately 20% of the cells were separated to perform flow cytometric analysis, as described above, to verify viability and determine cell counts, for the normalization of mass spectrometry data. The remaining cells were centrifuged for 3 minutes at 2000 rpm and supernatans was aspirated. The cell pellet was deproteinized using perchloric acid, followed by derivatization with o-phenylenediamine and quantification of MGO, glyoxal (GO), and 3-deoxyglucocone (3-DG) was performed as described previously (48).

Statistics – The normality was checked using the Shapiro-Wilk test. Normal distributed data were analysed with one-way or two-way ANOVA. For all data, multiple comparison was performed. Statistical analyses were performed with a confidence level of $\alpha = 0.05$ using GraphPad Prism 10. For measurements in triplicate or more, data is presented as the mean ± SD with individual values.

RESULTS

A concentration of 5 µM MBo is optimal for intracellular MGO detection – To establish optimal conditions for intracellular MGO detection, an initial series of optimization experiments was performed using the MBo probe (Fig. 2). Isolated neutrophils were incubated with increasing concentrations of MBo (0.5, 1, 2.5, 5, and 10 µM), and probe performance was evaluated based on signal intensity, cell viability, and reproducibility. The viability remained stable for all concentrations, however, there is a reduction after stimulation with PMA (Fig. 2A-C). Low MBo concentrations (0.5-1 µM) resulted in weak fluorescence signals that were insufficient for reliable detection of intracellular MGO (Fig. 2D). The intermediate concentration of 5 µM, in contrast with 2.5 µM, provided a robust and reproducible fluorescence signal while maintaining acceptable neutrophil viability (Fig. 2D-F). A higher concentration (10 µM), however, did not lead to reproducible higher fluorescent signals compared to 5 µM MBo (Fig. 2E). The concentration of 5 µM was selected for subsequent experiments.

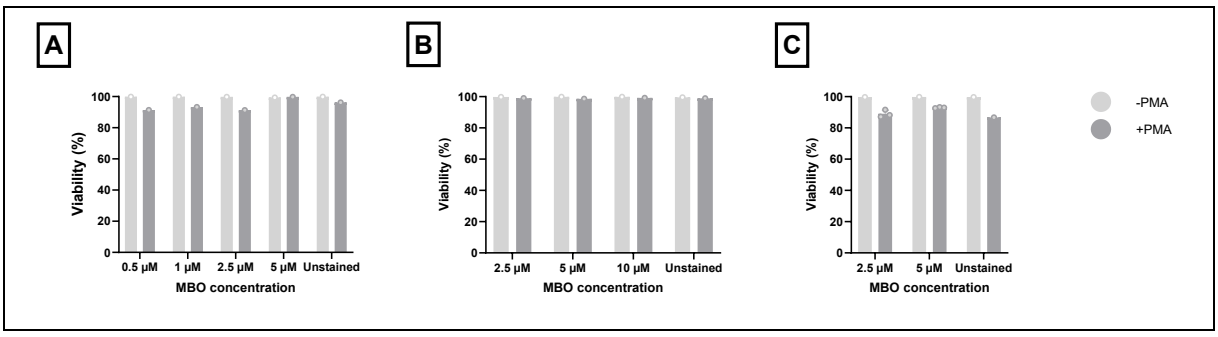

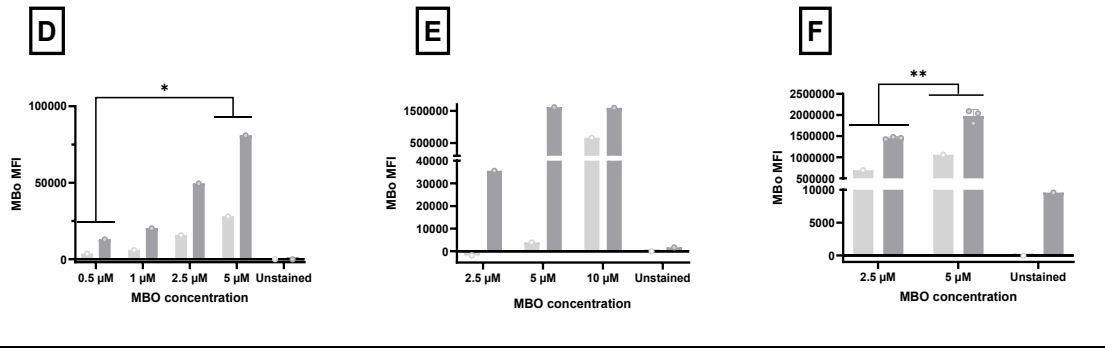

Fig. 2 – 5 µM is the most optimal MBo concentrations for intracellular MGO detection in neutrophils. Isolated neutrophils were pre-treated with varying concentrations of the MBo probe, stimulated (+PMA), and co-stained with Zombie NIR for viability assessment. Samples were analyzed via spectral flow cytometry. **(A-D)** Flow cytometric assessment of neutrophil viability following treatment with 0.5, 1, 2.5, 5 and 10 µM of the MBo probe. **(E-H)** Representative fluorescent signals detected from the MBo probe across the indicated concentration range. Data represent independent experiments conducted in single or triplicate replicates. For triplicate measurements, individual data points are presented with the mean ± SD. Two-way ANOVA with Tukey's multiple comparison was performed, with *p<0.05, **p<0.01. MBo, methyl diaminobenzene-BODIPY probe; MFI, mean fluorescence intensity; PMA, phorbol 12-myristate 13-acetate.

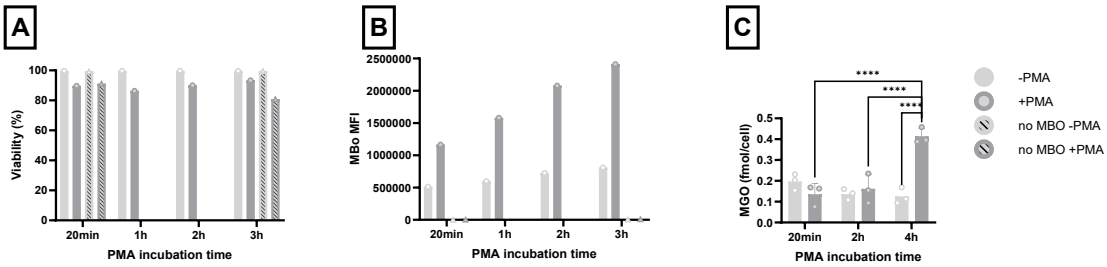

Fig. 3 – Validation of PMA-induced MGO production in neutrophils. Isolated neutrophils were stimulated (+PMA) over a time course of up to 4 hours to validate intracellular MGO production. **(A-B)** Flow cytometric quantification of viability (A) and intracellular MGO-associated fluorescence (B) using the MBo probe at 20 minutes, 1 hour, 2 hours, and 3 hours post-stimulation. **(C)** Quantification of intracellular MGO levels via mass spectrometry at 20 minutes, 2 hours, and 4 hours to validate the trends observed via flow cytometry. Data represent independent experiments performed in single or triplicate replicates. For triplicate measurements, individual values are presented with the mean ± SD. Statistical significance was determined by two-way ANOVA with Tukey's multiple comparison, with ****p<0.0001. CTRL, control; MBo, methyl diaminobenzene-BODIPY probe; MFI, mean fluorescence intensity; PMA, phorbol 12-myristate 13-acetate.

The optimal PMA incubation time for neutrophil stimulation is 4 hours – To determine the optimal experimental set-up for evaluating the MGO production following neutrophil activation with PMA, a time-course experiment was conducted. Initial validation was performed via flow cytometry utilizing the MBo fluorescent probe (Fig. 3A-B). Analysis of incubation periods ranging from 20 minutes to 3 hours demonstrated a time-dependent increase in MGO-associated fluorescence after PMA stimulation, with stable viability across all time periods. To further validate these findings and achieve absolute quantification, intracellular MGO levels were analyzed using liquid chromatography-mass spectrometry (Fig. 3C). The experimental window was extended to 4 hours to capture late-stage metabolic shifts. Consistent with the flow cytometric data, mass spectrometric analysis confirmed a significant rise in MGO concentrations over time in stimulated neutrophils. However, this rise is only seen after 2 hours, with a significant increase after 4 hours. After 20 minutes of PMA

incubation there is no increase in MGO levels seen on the mass spectrometer. Based on these results, 4 hours was identified as the optimal incubation period for subsequent experiments, balancing peak MGO production with cell viability.

Reduction of intracellular MGO levels using pharmacological intervention – To evaluate the efficacy of MGO-scavenging strategies, intracellular MGO levels were quantified in isolated neutrophils across various treatment conditions using flow cytometry and mass spectrometry (Fig. 4). The tested treatments include AG, a multi-compound cocktail (Res, Hes, and Pyr), its individual components, and the selective iNOS inhibitor 1400W (alone and in combination with AG). Flow cytometric analysis was used to assess cell viability (Fig. 4A, 4D, and 4F) and measure MBo-dependent fluorescence as a proxy for intracellular MGO levels (Fig. 4B, 4E, and 4G). Where indicated, these findings were cross-validated via mass spectrometry, with MGO levels normalized to absolute cell counts (Fig. 4C).

The initial experiment assessed AG treatment across 1-hour and 2.5-hour PMA stimulation periods (Fig. 4A-C). Neutrophil viability remained high across all conditions, with a significant reduction after PMA stimulation (Fig. 4A). A general reduction in MBo-associated fluorescence was observed in AG-treated samples compared to untreated controls (Fig. 4B). However, this inhibitory effect reached statistical significance only in unstimulated cells following a 2.5 hour incubation. Consistent with the optimization in Figure 3, a trend towards increased MGO production was noted at 2.5 hours compared to 1 hour of stimulation. Mass spectrometric analysis validated the decreasing trend of intracellular MGO-levels following AG treatment, though the reduction did not reach statistical significance (Fig. 4C).

Given the limited potency of AG, a multi-compound cocktail including Res, Hes, and Pyr, was evaluated using an extended 4-hour stimulation period to maximize detectable MGO accumulation (Fig. 4D-E). PMA stimulation induced a significant reduction in cell viability (Fig. 4D). This viability increased significantly after AG and cocktail treatment compared to the control in stimulated cells. Both interventions demonstrated a significant inhibitory effect on MGO-associated fluorescence (Fig. 4E). These results are currently being cross-validated using mass spectrometry for absolute quantification.

To elucidate the individual contributions of the cocktail components, Res, Hes, and Pyr were tested separately (Fig. 4F-G). Following a 4-hour stimulation, cell viability was significantly reduced by PMA, an effect that was exacerbated by Res treatment but mitigated by Pyr (Fig. 4F). Analysis of MGO levels revealed that Res and Hes independently induced a significant decrease in intracellular MGO, whereas Pyr treatment showed no effect (Fig. 4G). Mass spectrometric confirmation for these components is also currently in progress.

Based on the hypothesized interaction between AG and nitric oxide signaling, the iNOS inhibitor 1400W was evaluated. However, due to time constraints, this experiment was performed as a single pilot (n=1). Preliminary data (Fig. S2) exhibited inconsistencies regarding AG its effect compared to previous replicates. Consequently, these exploratory results were insufficient for a definitive conclusion.

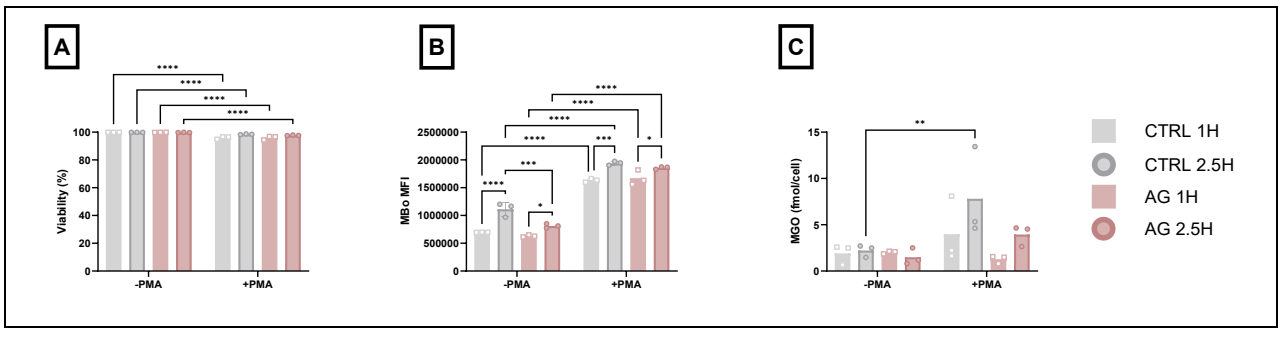

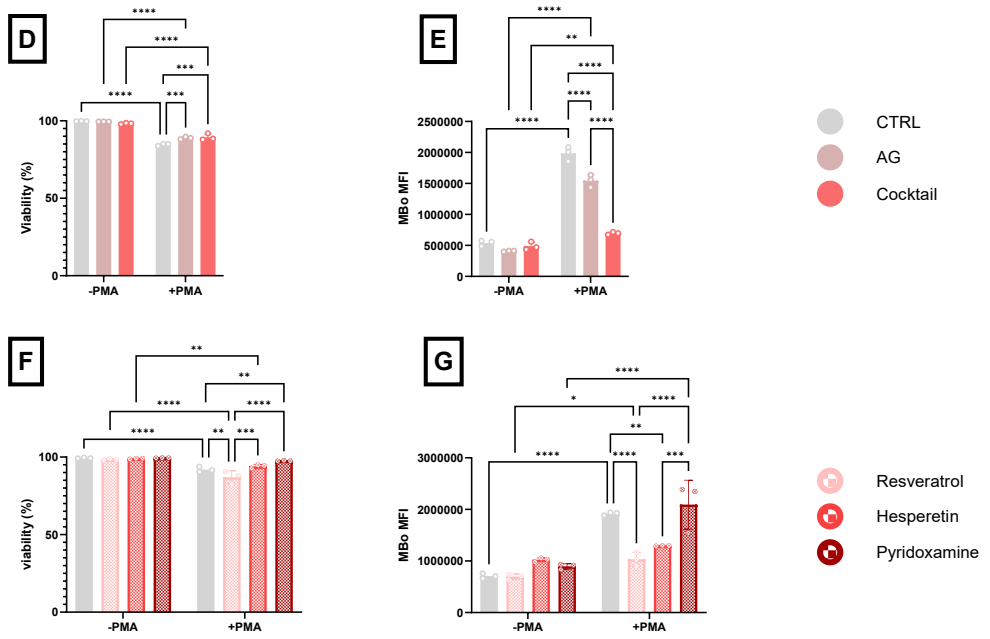

Fig. 4 – Effect of aminoguanidine (AG), a multi-compound cocktail, and its components on neutrophil intracellular MGO levels. Isolated neutrophils were treated with AG, a cocktail consisting of resveratrol (Res), hesperetin (Hes), and pyridoxamine (Pyr), or its separate components. Cells were stimulated (+PMA) for 1 hour, 2.5 hours or 4 hours prior to analysis. **(A, D, F)** Flow cytometric assessment of cell viability in neutrophils following AG treatment (A), AG or cocktail treatment (D), and Res, Hes, or Pyr treatment (F). **(B, E, G)** Flow cytometric evaluation of intracellular MGO-associated fluorescence in neutrophils following AG treatment (B), AG or cocktail treatment (E), and Res, Hes, or Pyr treatment (G). **(C)** Mass spectrometric quantification of intracellular MGO levels after AG treatment at 1 hour and 2.5 hours post-PMA stimulation. Three independent experiments were performed in triplicate. Data are presented as mean ± SD with individual values. Statistical significance was determined by two-way ANOVA with Tukey's multiple comparison, with *p<0.05, **p<0.01, ***p<0.001, and ****p<0.0001. AG, aminoguanidine; CTRL, control; H, hour; MBo, methyl diaminobenzene-BODIPY probe; MFI, mean fluorescence intensity; PMA, phorbol 12-myristate 13-acetate.

Therapeutical reduction of NETosis visualized by immunofluorescence microscopy – To evaluate whether MGO modulation affects neutrophil function, the impact of the treatments on NETosis was assessed with immunofluorescence microscopy (Fig. 5). Representative images visualize neutrophils under stimulated conditions (+PMA). An example of unstimulated neutrophils is indicated by a red arrow, while an example of stimulated cells is denoted by an orange arrow. All instances of NETosis are identified by white arrows. As expected, PMA stimulation induced NET formation (Fig. 5A). Quantitative morphometric analysis revealed that treatment with the multi-compound cocktail and Res attenuated both the percentage of NET formation and the proportion of stimulated neutrophils significantly (Fig. 5B-G). Hes also attenuated these percentages, however, this effect was weaker compared to the cocktail and Res. Pyr showed, in line with the MGO-level results, no effect. Interestingly, while AG successfully scavenged intracellular MGO (Fig. 4), it failed to inhibit NET formation following 4 hours of PMA stimulation (Fig. 5C), in the latest experiment it even increased the NETosis significantly (Fig. 5F). This suggests that while MGO reduction is a key feature of both interventions, the cocktail may target additional pathways required for the progression of NETosis that are not impacted by AG. Like previously mentioned, we hypothesized, based on literature, that AG also affects iNOS. Therefore, the iNOS inhibitor 1400W was also tested on NETosis. 1400W showed no effect, however, when combined with AG it showed a slight increase (Fig. 5F). Notably, the experiment of Fig. 5E-G was only performed once due to time restrictions.

Subcellular MGO localization is dependent on neutrophil activation stage – To investigate the intracellular distribution of MGO during neutrophil activation, confocal microscopy was employed on isolated neutrophils over a 5-hour time course (Fig. 6). In unstimulated (-PMA) cells, neutrophils maintained a typical lobulated nuclear morphology (blue) with myeloperoxidase (MPO, red) in azurophilic granules. Intracellular MGO is stained with the MBo probe (green), seen as granular puncta. Upon PMA stimulation, a decondensation of the nucleus and a progressive accumulation of MGO were observed. Notably, high-magnification analysis showed that MGO did not colocalize with MPO-positive granules. One hour and two hours post-stimulation, a further increase in MGO is seen. As the time course progressed toward four and five hours, significant morphological changes were evident, characterized by further nuclear decondensation and the expulsion of NETs. Over the time course of the stimulation, the MGO signal appeared to redistribute towards the outer side of the neutrophils.

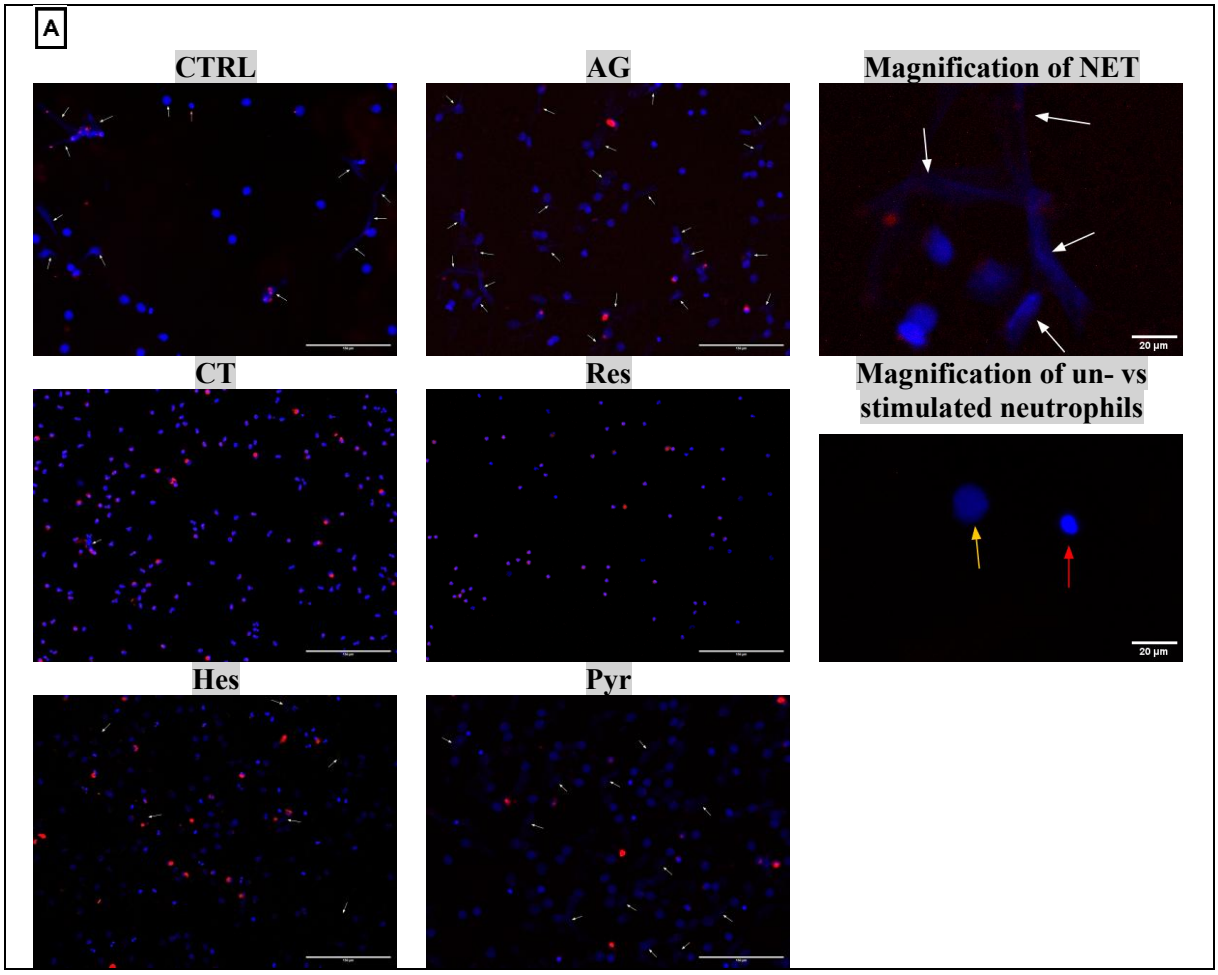

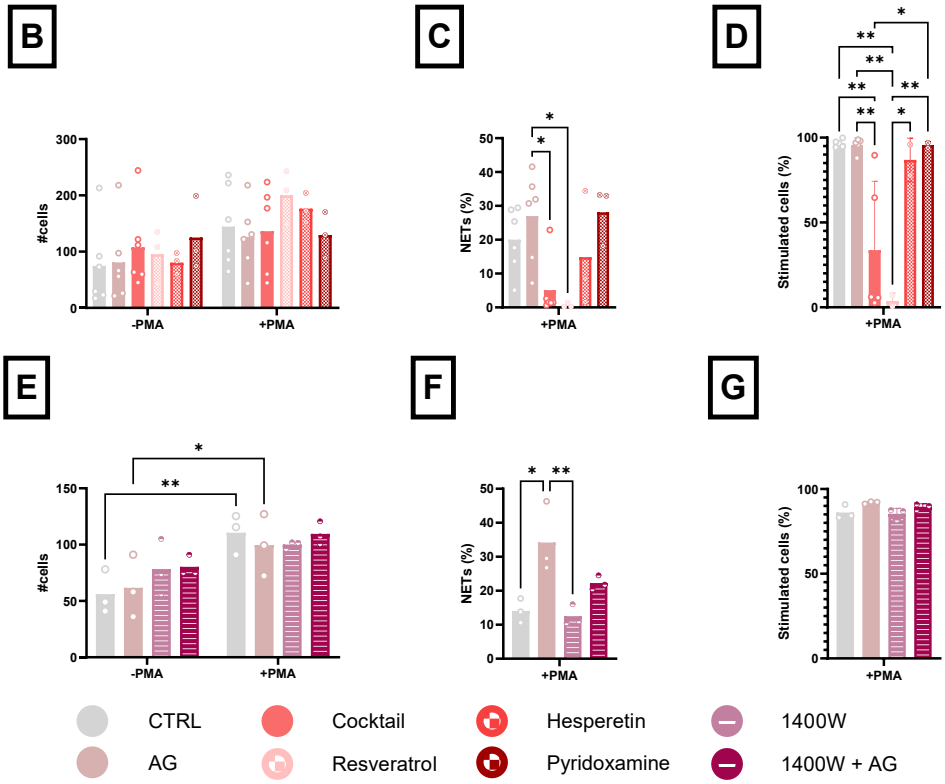

Fig. 5 – Effect of AG, a multi-compound cocktail, and its components on PMA-induced NETosis. Isolated neutrophils were pre-treated with AG, the cocktail (Res, Hes, and Pyr), or its components, and stimulated with PMA for 4 hours. Following fixation and immunofluorescence staining, NET formation was visualized via microscopy. **(A)** Representative immunofluorescent images of neutrophils under stimulated (+PMA) conditions with DAPI staining for the nucleus (blue) and MPO staining (red). NETosis is visualized with white arrows. An example of an unstimulated cell is identified by a red arrow, while an example of a stimulated cell is denoted by an orange arrow. **(B-G)** Quantitative morphometric analysis of total neutrophils (B, E), the percentage of NET-forming cells (C, F), and the percentage of stimulated neutrophils (D, G). Percentages were determined relative to the total neutrophil count per field of view. (B-D) Six independent experiments were performed in triplicate, three including the treatments AG and the cocktail and three including the same treatments and the separate components of the cocktail. (E-G) One experiment was performed in triplicate. Individual values are presented with the mean ± SD. Two-way ANOVA and one-way ANOVA with Tukey's multiple comparison were performed for the total neutrophil count and the percentages, respectively, with *p<0.05, and **p<0.01. AG, aminoguanidine; CT, multi-compound cocktail (resveratrol, pyridoxamine, and hesperetin); CTRL, control; Hes, Hesperetin; NET, neutrophil extracellular trap; PMA, phorbol 12-myristate 13-acetate; Pyr, pyridoxamine; Res, resveratrol.

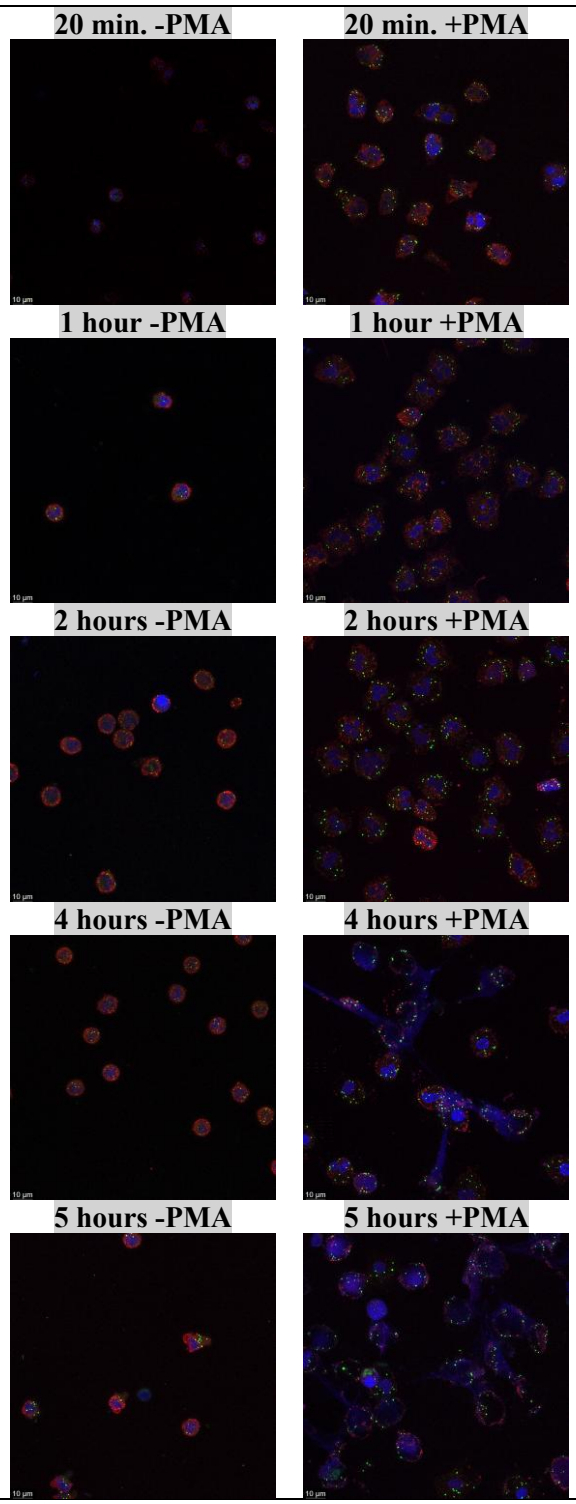

Fig. 6 – The localization of MGO within neutrophils. Representative confocal images showing the distribution of MGO (green, MBo probe) and MPO (red) in human neutrophils under stimulated (+PMA) and unstimulated (-PMA) conditions. Nuclei are counterstained with DAPI (blue). Isolated neutrophils were stimulated with PMA for 20 minutes, 1 hour, 2 hours, 4 hours or 5 hours. Two independent experiments were performed. PMA, phorbol 12-myristate 13-acetate.

DISCUSSION

This study aimed to investigate whether MGO production in human neutrophils modulates neutrophil inflammatory responses relevant to atherosclerotic cardiovascular disease in diabetes. Specifically, intracellular MGO levels, NETosis, and neutrophil morphology were assessed together with pharmacological interventions. Intracellular MGO formation was successfully detected in activated human neutrophils using flow cytometry and validated by mass spectrometry. NETosis was visualized using microscopy. Res and the multi-compound cocktail attenuated both intracellular MGO levels and NETosis. Hes also reduced both, but to a lesser extent compared to Res and the cocktail. Surprisingly, AG reduced the levels of MGO but failed to decrease the percentage of NETosis. This suggests that the mechanistic link between MGO and NETosis is not linear.

Mechanisms of MGO production and its role in NETosis – This study demonstrates that there is a significant increase in intracellular MGO upon activation of human neutrophils. Given that neutrophils rely predominantly on glycolysis for their energy demands, the enhanced glycolytic flux during activation likely drives the production of triose phosphates, specifically G3P and DHAP, which results in an increased non-enzymatic degradation into MGO (49). Mechanistically, our findings combined with literature suggest a self-amplifying inflammatory feedback loop within the activated cell. Our results demonstrate that PMA-stimulated neutrophils produce MGO, implicating PKC activation as an upstream trigger of MGO generation. Following the conversion of DAHP into diacylglycerol, PKC activation stimulates ROS production. This oxidative stress subsequently inhibits glyceraldehyde-3-phosphate dehydrogenase, blocking the conversion of G3P to pyruvate. This leads to an accumulation of glycolytic intermediates such as DHAP, favoring the spontaneous formation of MGO (18, 50, 51). Our findings therefore place neutrophil activation through PKC as a direct upstream event in MGO generation. The resulting MGO is known to promote the formation of AGEs, which trigger a pro-inflammatory cascade via NF-kB activation and downstream cytokine expression including IL-6 (49). Whether the oxidative stress and pro-inflammatory cytokines

produced through this mechanism are sufficient to induce NETosis remains to be tested in future research.

A central finding of this study was the superior efficacy of the cocktail compared to direct chemical quenching of AG and Pyr. Distinct mechanisms of action were observed among the tested pharmacological interventions. While Pyr and AG act as direct MGO scavengers, the flavonoids Hes and Res utilize a more complex cytoprotective signaling pathway (52-55). These compounds facilitate the dissociation of Nrf2 from its inhibitor KEAP1, allowing Nrf2 to translocate to the nucleus and bind to the antioxidant response element (ARE). This leads to the up-regulation of protective genes, most notably Glo1, which detoxifies MGO into D-lactate. Res likely enhances this process through the activation of SIRT1 (54, 55). Our results show that this indirect "metabolic priming", via the Nrf2/Glo1 axis and the inhibition of NF-kB, was more effective at reducing both MGO and NETosis than direct chemical quenching alone. The production of anti-oxidants and the inhibition of NF-kB leads to inhibition of ROS production and reduction of inflammation, respectively. As noted by Rabbani et al., chemical scavengers like AG often exhibit high off-target reactivity. In contrast, biological inducers provide a dual benefit, detoxifying MGO while simultaneously boosting the cell its antioxidant capacity (54, 55). This explains why the cocktail, Res, and Hes effectively inhibited both MGO accumulation and NETosis, whereas the effect of AG was inconsistent.

To validate these pathways, future research should evaluate the detoxification pathways and AGEs. Glo1 modulation can be measured through glyoxalase activity assays, western blotting, or qPCR (56). Nrf2 nuclear activity can be quantified using a luciferase reporter assay (57). Additionally, the metabolic product D-lactate can be quantified through an estimation kit or via lactate dehydrogenase activity (58). To further elucidate the pathway connecting the treatments with AGEs, AGE levels can be measured through UPLC-MS/MS, which would allow a precise characterization of AGE accumulation and its potential role in NETosis. Interestingly, a study of Junho et al. reported that AGE-modified albumin does not enhance NET formation, attributing this to low cell-surface expression of RAGE on neutrophils (59). However, this interpretation may be incomplete, as it does not account for the substantial intracellular RAGE pool, which could be engaged by intracellular MGO and result in NETosis (59, 60).

The aminoguanidine paradox – A striking finding was that AG successfully reduced MGO levels but simultaneously stimulated NETosis, contradicting our initial hypothesis. This suggests that the link between dicarbonyl stress and NETosis is not strictly linear. To our knowledge, no other studies have investigated NETosis using AG, making this a novel observation. This paradoxical effect may be explained by the pro-oxidative potential of AG under specific inflammatory conditions (61, 62). While AG scavenges MGO, it may also inadvertently promote the generation of ROS through activation of the NOX2 complex, that can stimulate the formation of NETs (39). AG is known to inhibit iNOS and to dissect the contribution of the iNOS pathway specifically, the selective iNOS inhibitor 1400W was assessed in the follow-up experiment. If AG its pro-NETotic effect was driven by iNOS inhibition, 1400W would be expected to recapitulate it. Instead, 1400W alone had no effect on NETosis compared to the control, but when combined with AG it reduced NETosis compared to AG alone. This partial rescue suggests that iNOS inhibition is not solely responsible for the increase in NETosis after AG treatment.

To further elucidate the connection between oxidative stress and these paradoxical findings of AG, future research should incorporate real-time ROS quantification. Utilizing flow cytometric probes such as DCFH-DA may provide critical insights into whether the AG-induced increase in NETosis is driven by an oxidative burst that bypasses the need for MGO-mediated signaling (56).

Synergistic attenuation of MGO by the multi-compound cocktail – Within the intervention groups, the cocktail and the component Res emerged as the most potent inhibitors of MGO and NETosis. While Res was the most effective in reducing NETosis, the cocktail resulted in lower MGO levels. This can be explained by the synergistic effect of the components. Res and Hes have a more proactive defense. They boost the cell its machinery to handle MGO before it accumulates by targeting the Nrf2/KEAP1 pathway to increase the

production of Glo1, while stimulating anti-oxidants that inhibit ROS production. Additionally, Pyr acts as an MGO-scavenger (52-55). Therefore, it seems possible that any MGO escaping from Glo1 can be chemically trapped by Pyr, which may reduce the MGO levels even more. However, in this study Pyr had no effect on MGO levels, contradicting its reported MGO-reducing effects, therefore this should be validated by investigating the cocktail with and without Pyr. It is also shown that Res works better than Hes although they both affect the Nrf2/KEAP1 pathway. This can be explained by the additional activation of SIRT1 by Res, which will inhibit NF-kB and therefore reduce inflammation (54, 55).

Intracellular localization of MGO – Confocal microscopy revealed a progressive accumulation and a distinct spatial redistribution of MGO following neutrophil activation. In resting neutrophils, MGO signal appeared diffuse and low, with some granular puncta visible. Upon PMA activation, MGO progressively accumulated and eventually translocated, potentially toward the cell periphery or areas of nuclear decondensation. MGO did not colocalize with MPO, arguing against an azurophilic granule origin. This suggests that MGO is metabolically derived from the cytosol or from other granular sources, like the secondary or tertiary granules. Therefore, future colocalization studies targeting for example lactoferrin and MMP-9 should be performed (63, 64).

This translocation suggests that MGO is not just a byproduct but a spatial participant in the NETosis process. First of all, MGO may translocate to areas where the nucleus is expanding or decondensing. This suggests that MGO may be directly interacting with chromatin (65, 66). MGO is known to react with the arginine and lysine residues of histones, reducing their positive charge and potentially weakening their bond with DNA. This facilitates the nuclear decondensation required for NETosis (65). Colocalization of MGO with CitH3, the gold standard marker for NETosis, would provide visual proof that MGO is present exactly where the DNA is being modified for release (67, 68).

Furthermore, MGO may have a peripheral movement, which suggests glycation of actin or tubulin. This glycation could drive the cytoskeletal remodeling necessary for the cell to flatten and eventually rupture (69). To validate this hypothesis, a staining of F-actin can be used in future experiments (70).

Future research – While this study establishes a clear foundation, some technical and physiological limitations must be recognized. First, the quantification of NETosis relied on a semi-quantitative approach based on morphological assessment and manual cell counting of neutrophils, stimulated neutrophils, and NETs. While this provides a foundational understanding of the NET formation and the inhibitory effects of our treatment, it is inherently subject to observer bias for both image acquisition and the subjective classification of cellular states. To enhance objectivity, sensitivity, and high-throughput capacity of future experiments, several alternative methodologies should be considered. To transition toward a more automated and objective quantification, an ELISA specifically optimized for the detection of NET-associated complexes could be utilized (71). Furthermore, measuring the enzymatic activity of NE through a functional activity assay would offer insights into the destructive potential of the released NETs (72). Finally, flow cytometry remains a powerful option for multi-parametric analysis. By utilizing specific markers for extracellular DNA and CitH3, objective gating and quantification of NETotic populations can be done in a high-throughput manner (73).

Additionally, PMA, a non-physiological, pharmacological stimulus, was used for the activation of neutrophils. PMA directly activates PKC, like mentioned above. This bypasses the cell surface receptors that a neutrophil would use in a human body. It triggers a maximal oxidative burst and NETosis, which can be an overestimation of the effect in the body (36). Future studies should therefore validate these findings using physiological stimuli such as LPS, or even high-glucose metabolic priming to see if the MGO-NETosis link remains under less extreme conditions (74).

Furthermore, clinical research shows that even when glycemic control is achieved, the CVD risk remains high due to metabolic memory (75). In this study neutrophils from healthy volunteers were used. Future studies need to investigate if the cocktail can erase this memory in neutrophils isolated from diabetic patients, whose cells have been epigenetically altered by years of dicarbonyl

stress. Healthy cells might react more rationally to treatments like the cocktail than cells from diabetic patients.

Lastly, future research that was mentioned throughout this discussion include the investigation of pathways including oxidative stress, pro-inflammatory cytokine signaling, AGEs, and detoxification, but also the comparison between the cocktail with and without Pyr, and stainings for the colocalization of MGO with lactoferrin, MMP-9, CitH3, and F-actin.

CONCLUSION

This study explored the role of MGO in human neutrophils and the functional outcomes regarding NETosis. By using flow cytometry and absolute mass spectrometric quantification, PMA-induced neutrophil activation is demonstrated to trigger a time-dependent accumulation of MGO, reaching peak levels after 4 hours of stimulation. Pharmacological investigations revealed that while the MGO-scavenger AG can reduce intracellular MGO levels, it failed to prevent the downstream process of NETosis visualized through immunofluorescence microscopy. In contrast, the flavonoids Res and Hes, particularly when combined in a multi-compound cocktail with Pyr, proved more effective at both reducing MGO-associated fluorescence and NETosis. These compounds function through the Nrf2/Glo1 signaling axis, enhancing the cell its capacity to detoxify MGO. Pyr treatment alone, however, did not reduce MGO levels or NETosis. This suggests that simply trapping MGO is insufficient if the intervention does not simultaneously address the oxidative burst that drives neutrophil rupture. Furthermore, the visualization of MGO its spatial redistribution, potentially towards the cell periphery and the decondensing nucleus, using confocal microscopy, suggests it is a functional participant in the NETosis process rather than a mere metabolic byproduct. The absence of colocalization with MPO indicates that MGO is not localized in azurophilic granules. For further localization, more research is necessary. In conclusion, these findings support the hypothesis that MGO accumulation drives neutrophil activation, however, other pathways such as oxidative stress, are also involved. This represents a critical mechanistic link between metabolic dysfunction and cardiovascular risk in diabetes that requires further investigation. Targeting these specific upstream metabolic drivers with a synergistic scavenging approach offers a promising strategy for mitigating the inflammatory damage that contributes to atherosclerotic cardiovascular disease in diabetes.

REFERENCES

1. N.A. The Diabetes Atlas International Diabetes Federation: Optima; 2025 [Available from: https://diabetesatlas.org/.
2. N.A. Diabetes Cleveland Clinic2023 [Available from: https://my.clevelandclinic.org/health/diseases/7104-diabetes.
3. Sun H, Saeedi P, Karuranga S, Pinkepank M, Ogurtsova K, Duncan BB, et al. IDF Diabetes Atlas: Global, regional and country-level diabetes prevalence estimates for 2021 and projections for 2045. Diabetes Res Clin Pract. 2022;183:109119.
4. Gregg EW, Sattar N, Ali MK. The changing face of diabetes complications. Lancet Diabetes Endocrinol. 2016;4(6):537-47.
5. Berezin A. Metabolic memory phenomenon in diabetes mellitus: Achieving and perspectives. Diabetes Metab Syndr. 2016;10(2 Suppl 1):S176-83.
6. N.A. What Is Cardiovascular Disease? American Heart Association2024 [Available from: https://www.heart.org/en/health-topics/consumer-healthcare/what-is-cardiovascular-disease.
7. N.A. Cardiovascular disease NHS2026 [Available from: https://www.nhs.uk/conditions/cardiovascular-disease/.
8. N.A. Cardiovascular disease Cleveland Clinic2022 [Available from: https://my.clevelandclinic.org/health/diseases/21493-cardiovascular-disease.
9. Brownlee M. The Pathobiology of Diabetic Complications: A Unifying Mechanism. Diabetes. 2005;54(6):1615-25.
10. Gimbrone MA, García-Cardeña G. Endothelial Cell Dysfunction and the Pathobiology of Atherosclerosis. Circulation Research. 2016;118(4):620-36.
11. Ridker PM. How Common Is Residual Inflammatory Risk? Circulation Research. 2017;120(4):617-9.
12. Baylis RA, Gomez D, Mallat Z, Pasterkamp G, Owens GK. The CANTOS Trial. Arteriosclerosis, Thrombosis, and Vascular Biology. 2017;37(11):e174-e7.
13. Ridker PM, Everett BM, Pradhan A, MacFadyen JG, Solomon DH, Zaharris E, et al. Low-Dose Methotrexate for the Prevention of Atherosclerotic Events. New England Journal of Medicine. 2019;380(8):752-62.
14. Wang G, Wang Y, Yang Q, Xu C, Zheng Y, Wang L, et al. Metformin prevents methylglyoxal-induced apoptosis by suppressing oxidative stress in vitro and in vivo. Cell Death Dis. 2022;13(1):29.
15. Hanssen NMJ, Westerink J, Scheijen J, van der Graaf Y, Stehouwer CDA, Schalkwijk CG. Higher Plasma Methylglyoxal Levels Are Associated With Incident Cardiovascular Disease and Mortality in Individuals With Type 2 Diabetes. Diabetes Care. 2018;41(8):1689-95.
16. Zhang X. Interplay of methylglyoxal and immune cells: implications for type 2 diabetes? : Maastricht University; 2023.
17. Vašková J, Kováčová G, Pudelský J, Palenčár D, Mičková H. Methylglyoxal Formation-Metabolic Routes and Consequences. Antioxidants (Basel). 2025;14(2).
18. Schalkwijk CG, Stehouwer CDA. Methylglyoxal, a Highly Reactive Dicarbonyl Compound, in Diabetes, Its Vascular Complications, and Other Age-Related Diseases. Physiological Reviews. 2020;100(1):407-61.
19. Schalkwijk CG, Micali LR, Wouters K. Advanced glycation endproducts in diabetes-related macrovascular complications: focus on methylglyoxal. Trends Endocrinol Metab. 2023;34(1):49-60.
20. Sun D, van Greevenbroek MMJ, Scheijen J, Kelly J, Schalkwijk CG, Wouters K. Methylglyoxal Mediates the Association Between 2-Hour Plasma Glucose and HbA1c With Inflammation: The Maastricht Study. J Clin Endocrinol Metab. 2025;110(7):2047-54.

21. Hanssen NM, Wouters K, Huijberts MS, Gijbels MJ, Sluimer JC, Scheijen JL, et al. Higher levels of advanced glycation endproducts in human carotid atherosclerotic plaques are associated with a rupture-prone phenotype. Eur Heart J. 2014;35(17):1137-46.
22. Dong G, Gan M, Xu S, Xie Y, Zhou M, Wu L. The neutrophil-lymphocyte ratio as a risk factor for all-cause and cardiovascular mortality among individuals with diabetes: evidence from the NHANES 2003-2016. Cardiovasc Diabetol. 2023;22(1):267.
23. Lai SL, Marín-Juez R, Stainier DYR. Immune responses in cardiac repair and regeneration: a comparative point of view. Cell Mol Life Sci. 2019;76(7):1365-80.
24. Peet C, Ivetic A, Bromage DI, Shah AM. Cardiac monocytes and macrophages after myocardial infarction. Cardiovasc Res. 2020;116(6):1101-12.
25. Paolisso P, Foà A, Bergamaschi L, Donati F, Fabrizio M, Chiti C, et al. Hyperglycemia, inflammatory response and infarct size in obstructive acute myocardial infarction and MINOCA. Cardiovasc Diabetol. 2021;20(1):33.
26. Jeon JH, Hong CW, Kim EY, Lee JM. Current Understanding on the Metabolism of Neutrophils. Immune Netw. 2020;20(6):e46.
27. Thind MK, Uhlig HH, Glogauer M, Palaniyar N, Bourdon C, Gwela A, et al. A metabolic perspective of the neutrophil life cycle: new avenues in immunometabolism. Front Immunol. 2023;14:1334205.
28. Adane T, Melku M, Worku YB, Fasil A, Aynalem M, Kelem A, et al. The Association between Neutrophil-to-Lymphocyte Ratio and Glycemic Control in Type 2 Diabetes Mellitus: A Systematic Review and Meta-Analysis. J Diabetes Res. 2023;2023:3117396.
29. Josefs T, Barrett TJ, Brown EJ, Quezada A, Wu X, Voisin M, et al. Neutrophil extracellular traps promote macrophage inflammation and impair atherosclerosis resolution in diabetic mice. JCI Insight. 2020;5(7).
30. Zhang S, Bories G, Lantz C, Emmons R, Becker A, Liu E, et al. Immunometabolism of Phagocytes and Relationships to Cardiac Repair. Front Cardiovasc Med. 2019;6:42.
31. Zhang X, Schalkwijk CG, Wouters K. Immunometabolism and the modulation of immune responses and host defense: A role for methylglyoxal? Biochim Biophys Acta Mol Basis Dis. 2022;1868(8):166425.
32. Ma Y. Role of Neutrophils in Cardiac Injury and Repair Following Myocardial Infarction. Cells. 2021;10(7).
33. Mesa MA, Vasquez G. NETosis. Autoimmune Dis. 2013;2013:651497.
34. Papayannopoulos V. Neutrophil extracellular traps in immunity and disease. Nature Reviews Immunology. 2018;18(2):134-47.
35. Wong SL, Demers M, Martinod K, Gallant M, Wang Y, Goldfine AB, et al. Diabetes primes neutrophils to undergo NETosis, which impairs wound healing. Nature Medicine. 2015;21(7):815-9.
36. Damascena HL, Silveira WAA, Castro MS, Fontes W. Neutrophil Activated by the Famous and Potent PMA (Phorbol Myristate Acetate). Cells. 2022;11(18).
37. Tian M, Qing C, Niu Y, Dong J, Cao X, Song F, et al. Effect of aminoguanidine intervention on neutrophils in diabetes inflammatory cells wound healing. Exp Clin Endocrinol Diabetes. 2013;121(10):635-42.
38. Thornalley PJ. Use of aminoguanidine (Pimagedine) to prevent the formation of advanced glycation endproducts. Archives of Biochemistry and Biophysics. 2003;419(1):31-40.
39. de Souza Ferreira C, Pennacchi PC, Araújo TH, Taniwaki NN, de Araújo Paula FB, da Silveira Duarte SM, et al. Aminoguanidine treatment increased NOX2 response in diabetic rats: Improved phagocytosis and killing of Candida albicans by neutrophils. European Journal of Pharmacology. 2016;772:83-91.

40. Lima TFO, Ferreira CdS, Araújo TH, Figueiredo SA, Paula FBdA, Duarte SMdS, et al. Aminoguanidine: effect on granular enzymes myeloperoxidase and elastase in human neutrophils / Aminoguanidina: efeito sobre as enzimas granulares mieloperoxidase e elastase em neutrófilos humanos. Brazilian Journal of Development. 2021;7(5):49395-414.
41. Magdaleno F, Blajszczak CC, Charles-Niño CL, Guadrón-Llanos AM, Vázquez-Álvarez AO, Miranda-Díaz AG, et al. Aminoguanidine reduces diabetes-associated cardiac fibrosis. Exp Ther Med. 2019;18(4):3125-38.
42. Jerums G, Soulis-Liparota T, Panagiotopoulos S, Cooper ME. In Vivo Effects of Aminoguanidine. In: Labuza TP, Reineccius GA, Monnier VM, O'Brien J, Baynes JW, editors. Maillard Reactions in Chemistry, Food and Health: Woodhead Publishing; 2005. p. 319-24.
43. DeGroot J. The AGE of the matrix: chemistry, consequence and cure. Current Opinion in Pharmacology. 2004;4(3):301-5.
44. Nelson M-AM, Baba SP, Anderson EJ. Biogenic Aldehydes as Therapeutic Targets for Cardiovascular Disease. Current Opinion in Pharmacology. 2017;33:56-63.
45. Salehi B, Mishra AP, Nigam M, Sener B, Kilic M, Sharifi-Rad M, et al. Resveratrol: A Double-Edged Sword in Health Benefits. Biomedicines. 2018;6(3).
46. Doki Y, Nakazawa Y, Morishita N, Endo S, Nagai N, Yamamoto N, et al. Hesperetin treatment attenuates glycation of lens proteins and advanced-glycation end products generation. Mol Med Rep. 2023;27(5).
47. Wang T, Douglass EF, Jr., Fitzgerald KJ, Spiegel DA. A "turn-on" fluorescent sensor for methylglyoxal. J Am Chem Soc. 2013;135(33):12429-33.
48. Scheijen JL, Schalkwijk CG. Quantification of glyoxal, methylglyoxal and 3-deoxyglucosone in blood and plasma by ultra performance liquid chromatography tandem mass spectrometry: evaluation of blood specimen. Clin Chem Lab Med. 2014;52(1):85-91.
49. Nigro C, Leone A, Fiory F, Prevenzano I, Nicolò A, Mirra P, et al. Dicarbonyl Stress at the Crossroads of Healthy and Unhealthy Aging. Cells. 2019;8(7).
50. Mirmiranpour H, Arden C. The Interplay Between Reactive Oxygen Species, Glucose Metabolism and NF-kB in the Pathogenesis of Type 2 Diabetes. Diabetology. 2026;7(3):53.
51. Inoguchi T, Sonta T, Tsubouchi H, Etoh T, Kakimoto M, Sonoda N, et al. Protein kinase C-dependent increase in reactive oxygen species (ROS) production in vascular tissues of diabetes: role of vascular NAD(P)H oxidase. J Am Soc Nephrol. 2003;14(8 Suppl 3):S227-32.
52. Thornalley PJ, Yurek-George A, Argirov OK. Kinetics and mechanism of the reaction of aminoguanidine with the alpha-oxoaldehydes glyoxal, methylglyoxal, and 3-deoxyglucosone under physiological conditions. Biochem Pharmacol. 2000;60(1):55-65.
53. Metz TO, Alderson NL, Thorpe SR, Baynes JW. Pyridoxamine, an inhibitor of advanced glycation and lipoxidation reactions: a novel therapy for treatment of diabetic complications. Arch Biochem Biophys. 2003;419(1):41-9.
54. Rabbani N, Thornalley PJ. Emerging Glycation-Based Therapeutics-Glyoxalase 1 Inducers and Glyoxalase 1 Inhibitors. Int J Mol Sci. 2022;23(5).
55. Zhu X, Liu Q, Wang M, Liang M, Yang X, Xu X, et al. Activation of Sirt1 by resveratrol inhibits TNF-α induced inflammation in fibroblasts. PLoS One. 2011;6(11):e27081.
56. Silvares RR, de Araujo BP, Pereira E, Rodrigues KL, Barbosa JMC, da Silva JF, et al. Pyridoxamine reduces inflammatory and microcirculatory abnormalities in metabolic dysfunction-associated steatohepatitis and modulates key factors in the hepatic AGE/ALE signaling pathway. Front Physiol. 2025;16:1736221.
57. Jiang T, Huang Z, Lin Y, Zhang Z, Fang D, Zhang DD. The protective role of Nrf2 in streptozotocin-induced diabetic nephropathy. Diabetes. 2010;59(4):850-60.
58. Awasthi D, Nagarkoti S, Sadaf S, Chandra T, Kumar S, Dikshit M. Glycolysis dependent lactate formation in neutrophils: A metabolic link between NOX-dependent and

independent NETosis. Biochimica et Biophysica Acta (BBA) - Molecular Basis of Disease. 2019;1865(12):165542.
59. Junho CVC, Dai Y, Schieren L, Hourtz S, Rykova T, Vondenhoff S, et al. Advanced glycation end product (AGE)-modified albumin does not enhance neutrophil extracellular trap formation and minimally impacts endothelial inflammation in large vessels. Life Sciences. 2026;398:124467.
60. Golenkina EA, Navarnova SV, Viryasova GM, Galkina SI, Gaponova TV, Romanova YM, et al. RAGE in Neutrophils: A Sensor for Pathogen-Associated Structures and Beyond. Biomedicines. 2026;14(5):1128.
61. Skamarauskas JT, McKay AG, Hunt JV. Aminoguanidine and its pro-oxidant effects on an experimental model of protein glycation. Free Radic Biol Med. 1996;21(6):801-12.
62. Philis-Tsimikas A, Parthasarathy S, Picard S, Palinski W, Witztum JL. Aminoguanidine Has Both Pro-oxidant and Antioxidant Activity Toward LDL. Arteriosclerosis, Thrombosis, and Vascular Biology. 1995;15(3):367-76.
63. Chakrabarti S, Zee JM, Patel KD. Regulation of matrix metalloproteinase-9 (MMP-9) in TNF-stimulated neutrophils: novel pathways for tertiary granule release. J Leukoc Biol. 2006;79(1):214-22.
64. Othman A, Sekheri M, Filep JG. Roles of neutrophil granule proteins in orchestrating inflammation and immunity. Febs j. 2022;289(14):3932-53.
65. Galligan JJ, Wepy JA, Streeter MD, Kingsley PJ, Mitchener MM, Wauchope OR, et al. Methylglyoxal-derived posttranslational arginine modifications are abundant histone marks. Proc Natl Acad Sci U S A. 2018;115(37):9228-33.
66. Zheng Q, Omans ND, Leicher R, Osunsade A, Agustinus AS, Finkin-Groner E, et al. Reversible histone glycation is associated with disease-related changes in chromatin architecture. Nature Communications. 2019;10(1):1289.
67. Mauracher LM, Posch F, Martinod K, Grilz E, Däullary T, Hell L, et al. Citrullinated histone H3, a biomarker of neutrophil extracellular trap formation, predicts the risk of venous thromboembolism in cancer patients. J Thromb Haemost. 2018;16(3):508-18.
68. Wang Y, Li M, Stadler S, Correll S, Li P, Wang D, et al. Histone hypercitrullination mediates chromatin decondensation and neutrophil extracellular trap formation. J Cell Biol. 2009;184(2):205-13.
69. Krishnamoorthi S, Saravanakumar R, Kumar V. Glycation at the Crossroads of Disease Pathogenesis: Mechanistic Insights and Therapeutic Frontiers. Diseases. 2026;14(4):137.
70. Shubhrasmita Sahu S, Sarkar P, Chattopadhyay A. Quantitation of F-actin in cytoskeletal reorganization: Context, methodology and implications. Methods. 2024;230:44-58.
71. Matta B, Battaglia J, Barnes BJ. A New Methodology for the Quantification of Neutrophil Extracellular Traps in Patient Plasma. Bio Protoc. 2023;13(12):e4701.
72. Wang Y, Xiao Y, Zhong L, Ye D, Zhang J, Tu Y, et al. Increased Neutrophil Elastase and Proteinase 3 and Augmented NETosis Are Closely Associated With β-Cell Autoimmunity in Patients With Type 1 Diabetes. Diabetes. 2014;63(12):4239-48.
73. Poli V, Di Gioia M, Zanoni I. Quantitative cytofluorimetric analysis of mouse neutrophil extracellular traps. STAR Protoc. 2023;4(3):102372.
74. Pieterse E, Rother N, Yanginlar C, Hilbrands LB, van der Vlag J. Neutrophils Discriminate between Lipopolysaccharides of Different Bacterial Sources and Selectively Release Neutrophil Extracellular Traps. Front Immunol. 2016;7:484.
75. Dong H, Sun Y, Nie L, Cui A, Zhao P, Leung WK, et al. Metabolic memory: mechanisms and diseases. Signal Transduction and Targeted Therapy. 2024;9(1):38.
This text was supported by GenAI

Acknowledgements – I would like to thank C.S. and K.W. for providing the opportunity to do my senior internship. I am grateful to R.K. and B.B. for training me in the NETosis assay and for granting access to the required materials and facilities. I would like to thank Y.O. for her assistance with experiments. I also thank S.D. and H.K. for their valuable advice and practical assistance regarding microscopy. J.S. and M.v.d.W. are thanked for performing the mass spectrometry experiments and providing the data. Special thanks go to K.W. for continuous guidance throughout the internship and for support during the writing of this thesis. Finally, I would like to thank T.S. for optimizing experimental protocols that were instrumental for this work.

Author contributions – M.V. and K.W. conceived and designed the research. M.V. performed experiments and data analysis. J.S performed mass spectrometry experiments. M.V. wrote the paper. K.W. revised and gave feedback on the paper. All authors carefully edited the manuscript.

Supplements

Statistics Table 1
MBO experiment-MBO experiment 1-10 uM AG +PMA

Gate	Count	% Parent	% Grand Parent	% Total	Median FITC-A	Median FSC-A	Median SSC-A
All Events	9,121	100.00	100.00	100.00	8,270	1,311,244	229,824
cells of interest	2,480	27.19	27.19	27.19	88,505	1,701,931	2,007,189
all alive	2,439	98.35	26.74	26.74	87,569	1,700,011	1,996,531
singlets 1	2,102	86.18	84.76	23.05	82,479	1,668,452	1,891,995
P1	2,073	98.62	84.99	22.73	82,493	1,669,600	1,879,631
P2	319	15.39	15.18	3.50	78,118	1,674,421	1,729,129
singlets 2	2,101	86.14	84.72	23.03	82,607	1,670,495	1,889,827
NOT	271	11.11	10.93	2.97	181,934	3,387,690	3,956,759
P3	163	60.15	6.68	1.79	174,175	3,371,151	3,493,114
P4	6	3.68	2.21	0.07	203,164	3,402,776	3,175,893

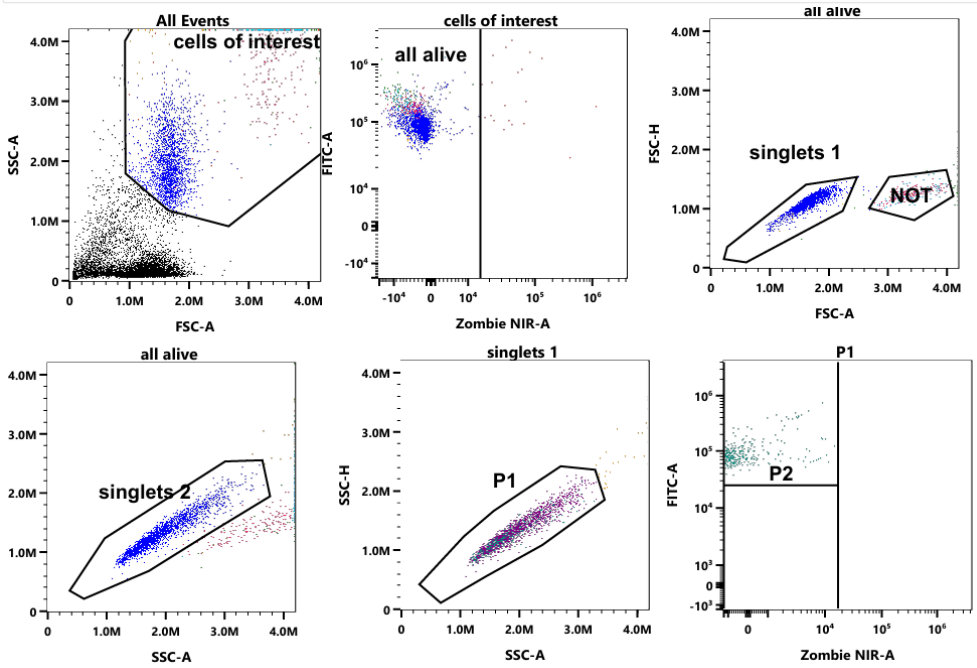

Figure S1: gating strategy for flow cytometry.

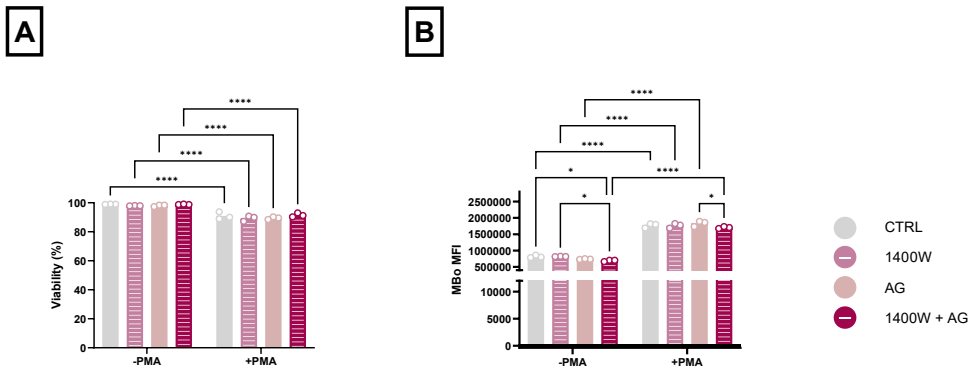

Fig. S2 – Effect of 1400W, aminoguanidine (AG), and the combination of both on neutrophil intracellular MGO levels. Isolated neutrophils were pre-treated with the MBo probe and treated with 1400W, AG, or a combination of 1400W and AG. Cells were stimulated with PMA for 4 hours prior to analysis. **(A)** Flow cytometric assessment of cell viability in neutrophils following treatments. **(B)** Flow

cytometric evaluation of intracellular MGO-associated fluorescence in neutrophils following treatments. Data are presented as individual values. Statistical significance was determined by two-way ANOVA with Tukey's multiple comparison, with *p<0.05, and ****p<0.0001. CTRL, control; PMA, phorbol 12-myristate 13-acetate; AG, aminoguanidine; MBo, methyl diaminobenzene-BODIPY probe; MFI, mean fluorescence intensity.